PHYSICAL REVIEW B VOLUME 61, NUMBER 12 15 MARCH 2000-II

Transport properties of strongly correlated metals: A dynamical mean-field approach

Jaime Merino* and Ross H. McKenzie†
School of Physics, University of New South Wales, Sydney 2052, Australia
(Received 8 September 1999)

The temperature dependence of the transport properties of the metallic phase of a frustrated Hubbard model on the hypercubic lattice at half-filling is calculated. Dynamical mean-field theory, which maps the Hubbard model onto a single impurity Anderson model that is solved self-consistently, and becomes exact in the limit of large dimensionality, is used. As the temperature increases there is a smooth crossover from coherent Fermi liquid excitations at low temperatures to incoherent excitations at high temperatures. This crossover leads to a nonmonotonic temperature dependence for the resistance, thermopower, and Hall coefficient, unlike in conventional metals. The resistance smoothly increases from a quadratic temperature dependence at low temperatures to large values which can exceed the Mott-Ioffe-Regel value $\hbar a/e^2$ (where a is a lattice constant) associated with mean free paths less than a lattice constant. Further signatures of the thermal destruction of quasiparticle excitations are a peak in the thermopower and the absence of a Drude peak in the optical conductivity. The results presented here are relevant to a wide range of strongly correlated metals, including transition metal oxides, strontium ruthenates, and organic metals.

I. INTRODUCTION

The discovery of heavy fermion metals, metal-insulator transitions in transition metal oxides, high-temperature superconductivity in copper oxides, and colossal magnetoresistance in manganates has stimulated extensive theoretical studies of strongly correlated electron models.[1,2] In spite of intensive research over the past decade the nature of the metallic state in strongly correlated materials is still poorly understood. This is particularly true of the cuprate superconductors, for which most of the metallic properties cannot be understood within the Fermi liquid picture that has so successfully described conventional metals.[3] Yet there are also a wide range of materials that have low-temperature properties (e.g., the observation of magnetic oscillations such as the de Haas–van Alphen effect) consistent with a Fermi liquid but which at higher temperature are inconsistent with a Fermi liquid. These include transition metal oxides,[4] heavy fermions,[5–7] strontium ruthenates,[8] the quasi-two-dimensional molecular crystals κ-(BEDT-TTF)$_2X$,[9] and the quasi-one-dimensional Bechgaard salts[10] (TMTSF)$_2X$ [BEDT-TTF=bis(ethylenedithio)-tetrathiafulvalene TMTSF =tetramethyltetraselenafulvalene]. In conventional metals the electronic properties are robust up to temperatures of some sizable fraction of the Fermi energy. In contrast, in the above materials the electronic properties change at some temperature much less than the Fermi energy.

A brief summary is now given of some of the common differences between the transport properties of strongly correlated metals and the properties of elemental metals. Later in the paper specific references will be given to experimental results on a wide range of materials.

Resistivity. Boltzmann transport theory gives an expression for the magnitude of the resistivity in terms of band parameters and a mean free path between quasiparticle collisions. At low temperatures this expression suggests a mean free path that is much larger than a lattice constant, as in conventional metals. However, at higher temperatures the resistivity smoothly increases to large values that suggest a mean free path smaller than a lattice constant, implying the breakdown of a quasiparticle picture.

Thermopower. In conventional metals this is linear in temperature, has values much lower than $k_B/e \simeq 87\ \mu$V/K, and has the same sign as the charge carriers. In strongly correlated metals it can have a nonmonotonic temperature dependence, can change sign, and can have values of the order k_B/e.

Hall resistance. In conventional metals this is weakly temperature dependent and gives the sign of the charge carriers. In strongly correlated metals, the Hall resistance can be strongly temperature dependent, change sign, and have the opposite sign to the thermopower.

Optical conductivity. In conventional metals, one observes a Drude peak at zero frequency, which broadens but persists to high temperatures. The spectral weight of this peak is comparable to that predicted from the optical sum rule and the density of charge carriers (or the plasma frequency). In contrast, in strongly correlated metals most of the spectral weight is in broad features at high energies. Furthermore, the Drude peak only exists at low temperatures.

A. Dynamical mean-field theory

The main purpose of this paper is to show that transport properties such as those described above are obtained in a dynamical mean-field treatment of the Hubbard model. Over the past decade a considerable amount of work has been done using this approximation to understand the Mott-Hubbard metal-insulator transition.[11,12] This approximation becomes exact in the limit of either large lattice connectivity or spatial dimensionality. It has been found to give a good description of three-dimensional transition metal oxides and has been argued to be relevant to the properties of the cuprates.[13,14] Whereas most previous studies of transport properties[13–17] have focused on doped Mott insulators we consider the case where the band is half filled and the Hubbard interaction U is less than the minimum value needed for

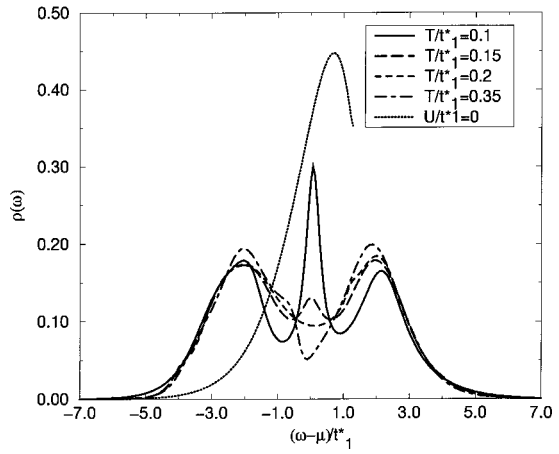

FIG. 1. Strong temperature dependence of the spectral density of the strongly correlated metallic phase of a Hubbard model at half-filling and in large dimensions. Note that only at the low temperatures does a coherent quasiparticle band form near the chemical potential μ. The broad features near $\omega-\mu\simeq\pm U/2$ are the lower and upper Hubbard bands. The results shown are for $U=4t_1^*$ and a degree of magnetic frustration of $t_2^*=0.3t_1^*$. For comparison we also show the noninteracting density of states ($U=0$), for which the square-root singularity placed at the upper band edge is not plotted. It is this strong temperature dependence of the spectral density that leads to many of the unconventional transport properties discussed in this paper.

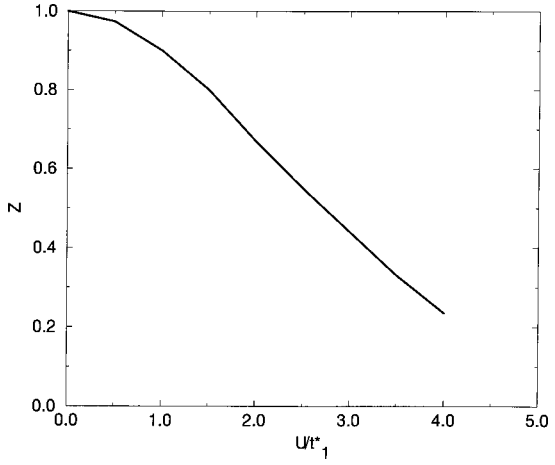

FIG. 2. Dependence of the Fermi liquid quasiparticle weight Z on the Hubbard interaction U. This paper focuses on the case of moderate interactions, $2<U/t_1^*<4$, corresponding to effective mass enhancements ($m^*/m_b=1/Z$) of 2–4, as observed in many organic metals (Refs. 9 and 38) and Sr_2RuO_4 (Ref. 39). Even for such moderate interactions the transport properties turn out to be strongly temperature dependent. The curves shown are for $t_2^*=0.1t_1^*$, but virtually identical results are obtained for $t_2^*=0.3t_1^*$.

the formation of the Mott insulating state. This is the situation in the metallic phase of the molecular crystals κ-(BEDT-TTF)$_2X$.[9]

Dynamical mean-field theory maps the Hubbard model onto a single impurity Anderson model that must be solved self-consistently. While time-dependent fluctuations are captured by this approximation, spatially dependent fluctuations are neglected. Some important physics that emerges[12] is that there is a low-energy scale T_0 which is much smaller than the noninteracting half-bandwidth D and the Coulomb repulsion U. D is of the order of the Fermi energy given by band structure calculations. This energy scale T_0 is the analog of the Kondo temperature for the impurity problem and defines the energy scale of coherent spin excitations. In the metallic phase the density of states $\rho(\omega)$ contains peaks at energies $\omega=-U/2$ and $+U/2$ which correspond to the lower and upper Hubbard bands, respectively, and involve incoherent charge excitations. These peaks are broad and have width of order D. At temperatures below T_0 a quasiparticle peak with width of order T_0 forms at the Fermi energy (see Fig. 1). The quasiparticle band involves coherent excitations (i.e., they have a well-defined dispersion relation) that form a Fermi liquid. The spectral weight of this peak (see Fig. 2) vanishes as the metal-insulator transition is approached. Thus, the temperature T_0 defines an energy scale at which there is a crossover from Fermi liquid behavior to incoherent excitations. A similar crossover occurs in heavy fermion materials.[5–7]

B. Overview

In Sec. II A the model we study is introduced: a Hubbard model on the hypercubic lattice with one electron per site (i.e., at half-filling). As well as a nearest-neighbor hopping t_1 a next-nearest-neighbor hopping t_2 is also included for several reasons. First, this term introduces magnetic frustration which enhances the stability of the metallic phase by suppressing the Néel temperature for antiferromagnetic ordering.[12] Second, in the absence of this term the model has exact particle-hole symmetry and the thermopower and Hall conductivity vanish. Third, the model represents a higher-dimensional version of a frustrated Hubbard model that describes the organic conductors κ-(BEDT-TTF)$_2X$.[9] In Sec. II B we review how the dynamical mean-field theory reduces to an impurity problem. In the infinite-dimensional limit all the vertex corrections to correlation functions vanish and transport quantities are determined by the one-electron spectral function. The relevant expressions are presented in Sec. II C. Section II D describes how the local impurity problem is solved at the level of iterated perturbation theory. This method is known to give reliable results for the impurity problem up to moderate interactions.

At low temperatures and low energies the electron self-energy has a Fermi liquid form and in Sec. III we present analytical results for the different transport quantities in this regime. An expression is derived for the Kadowaki-Woods ratio: the ratio of the T^2 coefficient of the resistivity to the square of the linear specific heat coefficient γ. For strong interactions it is shown to be independent of the band parameters and the strength of the interactions. The ratio of the thermopower to γT is shown to be independent of the strength of the interactions.

The temperature dependence of the different transport quantities is presented in Sec. IV. In particular we focus on the effect of the crossover from coherent to incoherent excitations with increasing temperature. For moderate to strong interactions the resistivity smoothly increases from a T^2 dependence at low temperatures to large values corresponding to mean free paths less than a lattice constant. For strong interactions the resistivity can have a nonmonotonic tem-

perature dependence; at temperatures several times the coherence temperature it decreases with increasing temperature. The thermopower is linear in temperature up to a temperature of the order of the coherence temperature at which it decreases. The resulting peak is similar to the peak that occurs in the electronic specific heat and is associated with the thermal destruction of the quasiparticles. For strong interactions most of the spectral weight in the optical conductivity is associated with transitions from (to) the lower (upper) Hubbard band. A Drude peak only exists for temperatures less than the coherence temperature.

II. DYNAMICAL MEAN-FIELD THEORY

A. The model

We consider a Hubbard model with nearest-neighbor hopping, t_1, and next-nearest-neighbor hopping, t_2, on a given lattice. The Hamiltonian is

$$H=t_1\sum_{ij,\sigma}(c^{\dagger}_{i\sigma}c_{j\sigma}+\text{H.c.})+t_2\sum_{ik,\sigma}(c^{\dagger}_{i\sigma}c_{k\sigma}+\text{H.c.})+U\sum_i n_{i\uparrow}n_{i\downarrow}-\mu\sum_{i\sigma}n_{i\sigma} \tag{1}$$

where U is the Coulomb repulsion between two electrons on the same site and μ is the chemical potential. We will only consider the case of half-filling, i.e., one electron per site. We treat the case of a d-dimensional hypercubic lattice with connectivity z, which has t_1 hopping to any of the $2z$ ($z=2d$) neighbors and t_2 along the diagonals of the elementary unit cell. In order to have a finite kinetic energy in the $d\to\infty$ limit the hoppings are rescaled as $t_1^*=\sqrt{2z}t_1$ and $t_2^*=\sqrt{2z(z-1)}t_2$, with $z=2d$, z being the connectivity of the lattice. The noninteracting ($U=0$) density of states, $D_0(\epsilon)=\Sigma_k\delta(\epsilon-\epsilon_k)$, associated with this lattice in the limit of infinite dimensions ($d\to\infty$) reads[18,12]

$$D_0(\epsilon)=\left(\frac{2}{\pi}\right)^{1/2}\frac{1}{E(\epsilon)}\cosh\left(\frac{E(\epsilon)t_1^*}{2t_2^{*2}}\right)\exp\left(\frac{t_1^{*2}-E(\epsilon)^2}{4t_2^{*2}}\right) \tag{2}$$

with $E(\epsilon)=(t_1^{*2}+2t_2^{*2}-2\sqrt{2}t_2^*\epsilon)^{1/2}$. $D_0(\epsilon)=0$, whenever $E(\epsilon)$ is not real. Note that $D_0(\epsilon)$ has a finite band edge with a square-root divergence. We set t_1^* as the unit of energy. The reason for choosing this lattice is that we can treat a varying degree of frustration by tuning the ratio t_2^*/t_1^*, which changes the shape of the bare density of states. Other lattices, such as the Bethe lattice with next-nearest neighbors, can also be used, but its density of states remains symmetric and therefore is qualitatively the same as its nonfrustrated counterpart. Before considering how this model can be studied using dynamical mean-field theory, we note a possible alternate approach to that used here. If one is interested in weak to intermediate values of U/t, one can directly start from a weak-coupling treatment of the infinite dimensional model. Such an approach was taken in Schweitzer's and Czycholl's[19] treatment of transport properties for the periodic Anderson model.

B. Local impurity self-consistent approximation

In the limit of infinite dimensions, mean-field theory of the full interacting lattice problem becomes exact and the problem reduces to solving a set of dynamical mean-field equations.[11,12] Therefore, the original Hubbard model is mapped to an impurity problem in the presence of a bath of electrons which describes the rest of the lattice electrons and that has to be found self-consistently. More precisely, one has to solve the associated single impurity Anderson model:

$$H=\sum_{k,\sigma}(\epsilon_k-\mu)c^{\dagger}_{k\sigma}c_{k\sigma}+\sum_{\sigma}(\epsilon_d-\mu)n_{d\sigma}+\sum_{k,\sigma}V_{kd}(c^{\dagger}_{d\sigma}c_{k\sigma}+c^{\dagger}_{k\sigma}c_{d\sigma})+Un_{d\uparrow}n_{d\downarrow}, \tag{3}$$

where the parameters ϵ_k and V_{kd} describe the bath of electrons through the hybridization function, which is defined as

$$\Delta(i\omega_n)=\sum_k\frac{|V_k|^2}{i\omega_n-\epsilon_k}. \tag{4}$$

This function represents the amplitudes for the lattice electrons to leave a site and, after wandering around the lattice, to return. Therefore the problem remains local in space coordinates but time-dependent correlations are fully taken into account. This is because in the large coordination limit, an electron can only hop once from one site to its nearest neighbor. Processes in which an electron can repeat a given path from one site to another in the lattice are suppressed as they are at least of order $1/d$. Some preliminary work is just appearing[20], that tries to extend the zero-order expansion to include this type of higher-order process.

The bath function $\Delta(i\omega_n)$ is determined self-consistently, from the following condition:

$$\Delta(i\omega_n)=i\omega_n-\Sigma(i\omega_n)-G^{-1}(i\omega_n), \tag{5}$$

where the self-energy $\Sigma(i\omega_n)$ is determined by solving the Anderson Hamiltonian (3), which is local in space, i.e., does not depend on momentum. $G(i\omega_n)$ is the lattice Green's function from which the spectral densities can be obtained,

$$\rho(\omega)=-\frac{1}{\pi}\text{Im}\,G(\omega+i\eta). \tag{6}$$

C. Transport quantities

In the limit of infinite dimensions, transport quantities can be calculated straightforwardly, due to the local nature of the self-energy. For example, the evaluation of the optical conductivity simplifies drastically as only the particle-hole bubble has to be evaluated in the Kubo formula. Contributions due to higher-order processes included in vertex corrections cancel exactly.[21] For a more detailed discussion of the derivation of the expressions presented here see Refs. 12 and 13.

Several transport quantities of interest can be obtained from the spectral density. The real part of the optical conductivity in the x direction is given by

$$\sigma_{xx}(\nu)=\sigma_0\int_{-\infty}^{\infty}d\omega\frac{f(\omega)-f(\omega+\nu)}{\nu}\frac{1}{N}\times\sum_{\mathbf{k}\sigma}\left(\frac{\partial\epsilon_{\mathbf{k}}}{\partial k_x}\right)^2\rho_{\mathbf{k}}(\omega)\rho_{\mathbf{k}}(\omega+\nu), \quad (7)$$

where a is the lattice constant, $\sigma_0=e^2\pi/2\hbar a$, and N is the total number of sites in the system.

In the low-frequency limit, $\nu\to 0$, the Hall conductivity reduces to

$$\sigma_{xy}^H=\sigma_0^H\int_{-\infty}^{\infty}d\omega\frac{\partial f(\omega)}{\partial\omega}\frac{1}{N}\sum_{\mathbf{k}\sigma}\left(\frac{\partial\epsilon_{\mathbf{k}}}{\partial k_x}\right)^2\frac{\partial^2\epsilon_{\mathbf{k}}}{\partial k_y^2}\rho_{\mathbf{k}}(\omega)^3, \quad (8)$$

where B is an external magnetic field that points in the z direction and $\sigma_0^H=2\pi^2|e|^3aB/3\hbar^2$. From the above equations we can evaluate the Hall coefficient, $R_H\equiv\sigma_{xy}/(\sigma_{xx}^2B)$. R_H can be derived from a more general expression[22] which correctly describes the high- and low-frequency limits. This generalized expression involves integrations all over the Brillouin zone which, for frequencies $\nu>\max(U,t)$, cannot be written as an integral over the Fermi surface such as the ones that appear in Eqs. (7) and (8). Therefore, the Hall coefficient we have computed remains valid only in the low-frequency limit. Calculations within dynamical mean-field theory using iterative perturbation theory (IPT) for the high-frequency Hall coefficient R_H^* have been carried out by Majumdar and Krishnamurthy[23] for the doped Mott insulator.

The thermopower is defined as

$$S=-\frac{k_B}{|e|T}\frac{L_{12}}{L_{11}}, \quad (9)$$

where the transport integrals reduce in the $d\to\infty$ limit to

$$L_{jk}=\int_{-\infty}^{\infty}d\omega\left(-\frac{\partial f(\omega)}{\partial\omega}\right)\left[\frac{1}{N}\sum_{k\sigma}\left(\frac{\partial\epsilon_k}{\partial k_x}\right)^2\rho_k(\omega)^2\right]^j\omega^{k-1}. \quad (10)$$

In the above expressions, a further simplification can be made in the case of a simple hypercubic lattice, as all sums in the momentum reduce to integrations in energy weighted by the density of states:

$$\frac{1}{N}\sum_{k\sigma}\left(\frac{\partial\epsilon_{\mathbf{k}}}{\partial k_x}\right)^2\rho_{\mathbf{k}}(\omega)^2=\frac{2}{d}\int_{-\infty}^{\infty}d\epsilon D_0(\epsilon)\rho(\epsilon,\omega)^2, \quad (11)$$

$$\frac{1}{N}\sum_{\mathbf{k}\sigma}\left(\frac{\partial\epsilon_{\mathbf{k}}}{\partial k_x}\right)^2\frac{\partial^2\epsilon_{\mathbf{k}}}{\partial k_y^2}\rho_{\mathbf{k}}(\omega)^3=-\frac{1}{2d^2}\int_{-\infty}^{\infty}d\epsilon D_0(\epsilon)\epsilon\rho(\epsilon,\omega)^3, \quad (12)$$

with the spectral densities given by

$$\rho(\epsilon,\omega)=-\frac{1}{\pi}\,\mathrm{Im}\left(\frac{1}{\omega+\mu-\epsilon-\Sigma(\omega+i\eta)}\right). \quad (13)$$

We will use this simplification in order to avoid the cumbersome sums over momentum. In particular the dc conductivity reduces to the following expression:

$$\sigma_{xx}=\frac{2\sigma_0}{d}\int_{-\infty}^{\infty}d\epsilon D_0(\epsilon)\int_{-\infty}^{\infty}d\omega\left(-\frac{\partial f(\omega)}{\partial\omega}\right)\rho(\epsilon,\omega)^2 \quad (14)$$

for the simple hypercubic lattice.

For reasons of simplicity, we will still use the above expressions in the presence of a nonzero t_2^*. This is because the focus of this paper is on many-body effects and not on how different band structures may change the results slightly.

D. Iterative perturbation theory

A wide range of techniques have been used to solve the Anderson model (3). An extensive review has been given by Hewson.[24] Among them the iterative perturbation theory is straightforward and at the same time gives a qualitatively correct description because it recovers exactly the atomic ($U/D\to\infty$) and the noninteracting ($U=0$) limits. It also provides a fast way of scanning a wide range of parameters in the Anderson model, which, by means of other methods such as exact diagonalization and quantum-Monte Carlo is computationally very demanding. Other approximate schemes such as the noncrossing approximation, which takes an infinite resummation of a certain class of perturbative diagrams, is limited in its applicability to high temperatures.[25]

Originally, the iterative perturbation scheme could be applied only for systems at half-filling and with particle-hole symmetry. This limitation comes from the fact that the high-energy behavior of the spectral density is exactly reproduced for half-filling by accident but this is not true at arbitrary filling. However, our main interest in this work is to study frustrated models where the noninteracting density of states is nonsymmetric and, consequently, particle-hole symmetry is broken. Recently Kajueter and Kotliar[26] have modified the standard iterative perturbation theory to treat asymmetric cases, based on the earlier work of Martin-Rodero *et al.*[27] by which the self-energy is built up as an interpolative solution that recovers both the strong- and weak-coupling limits and satisifies the Friedel-Langreth sum rule. Other authors[28] have extended this framework to compute more accurately the high-energy features of the spectral densities. Nevertheless, all of them approximately agree with exact diagonalization calculations when the interaction U is relatively large.

Our present work analyzes the transport properties of metals that are strongly correlated but sufficiently away from the Mott transition so that well-defined quasiparticles exist at low temperatures. This means that we are always in the metallic side of the Mott transition but not too close to the critical point at which the quasiparticle weight vanishes. Some controversy has arisen recently[29] on the reliability of IPT even for moderate couplings of the interaction. Müller-Hartman[30] and also Schweitzer and Czycholl[31] had earlier shown that a second-order expansion in terms of the skeleton diagrams which depend on the interacting Green's function, $G(i\omega_n)$ instead of $G^0(i\omega_n)$, does not reproduce the upper and lower Hubbard bands: only a Fermi liquid type peak is found in the spectral density. The skeleton diagrams enter the expansion of the Luttinger-Ward functional and are the ones that collapse into a local form as $d\to\infty$, giving a local self-energy.[11,12] However, Yamada[32] has shown that

when taking into account all the fourth order terms, the upper and lower Hubbard bands are reproduced, in agreement with the IPT results. This means that an expansion up to second order in the interacting Green's functions is insufficient to grasp the correct behavior of the spectral density. Moreover, recent nonperturbative calculations done by Bulla, Hewson, and Pruschke,[33] using the numerical renormalization group for the Hubbard model in infinite dimensions, clearly show the formation of the upper and lower Hubbard bands. Therefore, we believe that the method used here can be safely applied, giving a qualitative description of strongly correlated metals.

We use the finite-temperature version of the formalism, instead of the one used by Kajueter and Kotliar,[26] valid at $T=0$, as we are interested in the thermodynamic properties of correlated metals over a wide range of temperatures.

We briefly outline the method used and refer the reader to the more detailed work recently published.[26,34,28]

(i) Guess of an effective hybridization function $\Delta(i\omega_n)$ and input of the chemical potential of the system μ together with the chemical potential of the effective bath μ_0. We fix the population per site of the interacting lattice to be $n \equiv \langle n_\sigma \rangle = 0.5$, and it is kept fixed along the rest of the steps.

(ii) Computation of the Green's function of the effective bath

$$G_0(i\omega_n) = \frac{1}{i\omega_n + \mu_0 - \Delta(i\omega_n)} \tag{15}$$

and computation of the population of the bath $n_0 \equiv \langle n_{0\sigma} \rangle = -G_0(\tau = 0^-)$.

(iii) Ansatz for the self-energy, which is given by

$$\Sigma(i\omega_n) = Un + \frac{A\Sigma^{(2)}(i\omega_n)}{1 - B\Sigma^{(2)}(i\omega_n)} \tag{16}$$

with A and B defined as

$$A = \frac{n(1-n)}{n_0(1-n_0)} \quad B = \frac{U(1-n) - \mu + \mu_0}{U^2 n_0(1-n_0)}. \tag{17}$$

The second-order self-energy $\Sigma^{(2)}(i\omega_n)$ is computed from the imaginary time-dependent Green's function of the bath

$$\Sigma^{(2)}(i\omega_n) = \int_0^\beta d\tau e^{i\omega_n \tau} \Sigma(\tau) \tag{18}$$

where $\Sigma(\tau) = -U^2 G^0(\tau) G^0(\tau) G^0(-\tau)$. We use fast Fourier transforms to go back and forth from time to energy variables. The expression obtained for A, Eq. (17), comes from fixing the $m=2$ moment of the spectral density as explained in Ref. 28:

$$M^{(m)} = \int_{-\infty}^{\infty} w^m \rho(w) dw \tag{19}$$

where $M^{(m)}$ can be computed from the Heisenberg equations of motion. The parameter B is fixed from the exact atomic limit solution, $V_{kd} \to 0$.

(iv) Computation of the impurity Green's function

$$G(i\omega_n) = \sum_k G(i\omega_n, k) = \int_{-\infty}^{\infty} \frac{D_0(\epsilon) d\epsilon}{i\omega_n + \mu - \epsilon - \Sigma(i\omega_n)}. \tag{20}$$

The free parameters (μ_0, μ), can be now fixed from the following set of equations:

$$n = -G(\tau = 0^-) = 0.5,$$

$$n = n_0. \tag{21}$$

The last condition, originally introduced by Martin-Rodero *et al.*[27] together with the expressions for the interpolative self-energy (16) and (17), is nearly equivalent to the Luttinger condition or the Friedel-Langreth sum rule,[35] and fixes the correct low-energy behavior of the self-energy. Numerically this condition is much easier and faster to handle than the Luttinger one. Results from both of these conditions agree equally well with results from exact diagonalization of finite clusters.[28] Finding (μ_0, μ) takes around four to six iterations using Broyden's method.[36]

(v) The final step is the requirement that the lattice Green's funtion $G(i\omega_n)$ coincide with the Green's function of the associated impurity problem given by the Anderson Hamiltonian. This condition is expressed in Eq. (5).

The above steps (i)–(v) are repeated until a self-consistent bath function is obtained. Note that the calculations are kept on the imaginary frequency axis: this makes the computation much faster and more efficient with the use of fast Fourier transform algorithms. Analytical continuation to the real frequency axis is needed in order to compute the spectral densities entering the different transport quantities. This continuation is numerically implemented using Padé approximants.[37]

III. FERMI LIQUID BEHAVIOR AT LOW TEMPERATURES

For temperatures and frequencies much less than the Kondo temperature the self-energy $\Sigma(\omega)$ of the Anderson model has the Fermi liquid form[24]

$$\Sigma(\omega, T) = \omega\left(1 - \frac{1}{Z}\right) - iC[\omega^2 + (\pi k_B T)^2], \tag{22}$$

where Z is the quasiparticle weight and C is a positive constant. At sufficiently low temperatures and energies the imaginary part becomes much smaller than the bandwidth and the spectral function (13) will have well-defined peaks when $\omega = ZE_k$, where E_k is the band dispersion relation in the absence of interactions. The dependence of the quasiparticle weight Z on the Hubbard interaction U is shown in Fig. 2. The specific heat will be linear in temperature at low temperatures with a slope that is $1/Z$ times larger than the noninteracting value. The effective mass m^* deduced from magnetic oscillations will also be larger than m_b, the value predicted by band structure calculations, by the same factor $(m^*/m_b = 1/Z)$. This enhancement is found to be about two to four in many organic metals[9,38] and Sr_2RuO_4.[39] In this section we consider the low-temperature transport properties that follow from this form of the self-energy.

A. Resistivity

The resistivity in a Fermi liquid behaves as

$$\rho \simeq AT^2. \tag{23}$$

Such a temperature dependence is characteristic of metals in which the dominant scattering mechanism is the interaction of the electrons with one another and is observed in transition metals,[4] various organic conductors,[9] and heavy fermions.[5]

Yamada and Yosida[40] demonstrated this behavior for an Anderson lattice and showed that Umklapp scattering events should dominate the contribution to the resistivity because momentum conservation would give an infinite conductivity when the lattice is not present. Uhrig and Vollhardt have shown how in the limit of large dimensions the umklapp processes lead to a finite conductivity.[41] Cox and Grewe pointed out that in an anisotropic system when the electron velocity and momentum are no longer parallel normal scattering can contribute to the resistivity.[6]

In transition metals and heavy fermions the Kadowaki-Woods rule[42,43] relates the coefficient A to the linear coefficient for the specific heat, γ: $A/\gamma^2 = \text{const}$. The constant is 4.0×10^{-13} Ω cm $(\text{mol/mJ})^2$ for transition metals, and 1.0×10^{-11} Ω cm $(\text{mol/mJ})^2$ for most heavy fermions and for transition metal oxides near the Mott-Hubbard transition.[44] However, recent measurements on $UPt_{5-x}Au$ found values of 10^{-12} Ω cm $(\text{mol/mJ})^2$ for $x=0,0.5$ but increasing to 10^{-11} Ω cm $(\text{mol/mJ})^2$ for $x>1.1$.[45]

We now evaluate the ratio A/γ^2 using our results. From the self-energy (22), the resistivity in the low-temperature limit associated with expression (14) is

$$\rho(T) \simeq \frac{2d\sqrt{2\pi}k_B^2\hbar a}{e^2 D I_{01}} CT^2, \tag{24}$$

where we have numerically integrated

$$I_{nm} \equiv \int_{-\infty}^{\infty} \frac{dx x^n}{(x^2+\pi^2)^m} \frac{e^x}{(1+e^x)^2} \tag{25}$$

and find $I_{01} \simeq 1/12$. Expression (24) is the resistivity at low temperatures for the case of a simple hypercubic lattice, for which the density of states is $D_0(\epsilon) = (1/\sqrt{\pi}t_1^*)e^{-\epsilon^2/t_1^{*2}}$ and $t_1^{*2} = 4t_1^2 d$. D is the effective half-bandwidth defined as $D = \sqrt{2}t_1^*$.

The linear specific heat term for the same density of states is

$$\gamma = \frac{2\sqrt{2\pi}\pi k_B^2}{3ZD}, \tag{26}$$

where Z is the quasiparticle weight. Combining expressions (24) and (26) we obtain

$$\frac{A}{\gamma^2} = \frac{9d\sqrt{2\pi}\hbar a}{4\pi^3 k_B^2 I_{01} e^2} DCZ^2. \tag{27}$$

Hence, we see that if the dimensionless quantity DCZ^2 is universal then so will be the ratio A/γ^2. Insight into this question can be gained by considering first a pure Anderson model, for which we take a constant hybridization $\Delta = D$. For this case, it is found that[24] $C = (R-1)^2/2DZ^2$, where R is Wilson's ratio,

$$R = \frac{\chi_{loc}/\chi_{loc}^0}{\gamma/\gamma^0}, \tag{28}$$

and χ_{loc} is the local susceptibility, γ is the linear coefficient for the specific heat, and the zero superscript denotes the values in the absence of interactions. R takes values between 1 for $U=0$ and the universal value 2 for $|U/D| \geqslant 1$ (Kondo regime).[24]

TABLE I. Values of the fitting parameter C and quasiparticle weights for different values of the Coulomb repulsion U for the frustrated hypercubic lattice. Note that C scales with $1/Z^2$ even for values of the interaction such that the metallic phase has well defined quasiparticles with only moderate enhancements of the effective masses.

U/t_1^*	Ct_1^*	$Z(U)$	$CZ^2t_1^*$
1	0.1	0.9	0.08
1.5	0.23	0.8	0.16
2	0.44	0.67	0.20
2.5	0.70	0.55	0.21
3	1.07	0.45	0.22

We also find that this scaling holds for the Anderson model with the self-consistent bath. We found C by fitting the imaginary part of the self-energy obtained from our dynamical mean-field theory calculations to the low-frequency and low-temperature form (22), for different values of U. As shown in Table I, we find that C scales with $1/Z^2$ for $U \geqslant 2t_1^*$ as expected as we are in the Kondo regime, giving a universal behavior of the A/γ^2 ratio. However, it decreases for $U \leqslant 2$, consistent with the result from the Anderson model that $R \to 1$ in the $U \to 0$ limit.

From the numerical values of C in Table I, we can compute the A/γ^2 ratio, using the density of states of a simple hypercubic lattice: we get for $U \approx 3.0$ (Kondo regime) a ratio of $(1.24a)\times10^{-12}$ Ω cm. This result is comparable to experimental findings for transition metal oxides if we take the lattice constant to be $a \approx 10$ Å.

Previous calculations using a highly accurate projective method to solve the dynamical mean-field theory on the Bethe lattice find that very close to the Mott-Hubbard transition $A/\gamma^2 = (2.3a)\times10^{-12}$ Ω cm$(\text{mol/mJ})^2$ where a is the lattice constant in Å of a three-dimensional system at half-filling.[46] This differs from our result by a factor of 2 but turns out to be due to the different lattice used. In order to make a direct comparison with the results obtained in Ref. 46 we have repeated our calculations using iterative perturbation theory for a Bethe lattice at half-filling. We take a noninteracting density of states $D_0(\epsilon) = (1/t_1^*\pi)\sqrt{2-(\epsilon/t_1^*)^2}$. The fitting parameters of the self-energy to the low-temperature form for the Bethe lattice are shown in Table II. We find that already for moderate values of U, the value of CZ^2 converges rapidly to the value obtained in Ref. 46, providing a stringest test of the method used here.

TABLE II. The same as in Table I for the Bethe lattice. The final entry is the result obtained in Ref. 46 using a highly accurate projective method. $U_c = 4.13 t_1^*$ refers to the critical value at which the $T=0$ second order metal-insulator transition takes place.

U/t_1^*	Ct_1^*	$Z(U)$	$CZ^2 t_1^*$
1.5	0.35	0.72	0.18
2.0	0.70	0.57	0.23
2.5	1.40	0.42	0.25
$Uc = 4.13$			0.29

B. Thermopower

Similarly to the above analysis for the resistivity we can gain some insight into the behavior of the thermopower at low temperatures from the Anderson model. It can be shown for the N-fold degenerate Anderson model,[47] that the thermopower increases linearly with temperature at low temperatures. Its slope scales as $1/Z$, in the same way as the slope of the specific heat. Therefore, within the Anderson model the ratio of the thermopower to the linear coefficient of the specific heat is independent of Coulomb interaction. However, it depends on the band filling: it drops to zero as half-filling is reached, as it should, as for a system with particle-hole symmetry at half-filling the thermopower is zero.

The low-temperature behavior of the transport integral L_{12} defined in Eq. (10), can be shown to be

$$L_{12} = \left. \frac{\partial D_0(\epsilon)}{\partial \epsilon} \right|_{\epsilon=\epsilon_F} \frac{1}{2\pi Z C} I_{21} \tag{29}$$

where I_{21} is the integral defined by Eq. (25) and the term proportional to the bare density of states at the Fermi energy vanishes as the integral is antisymmetric. On the other hand, L_{11} is proportional to the dc conductivity and reduces for low temperatures to the T^2 behavior analyzed in Sec. III A. Therefore expression (9) reduces to

$$S(T) = \frac{-k_B}{|e|} \left. \frac{\partial D_0(\epsilon)/\partial \epsilon}{D_0(\epsilon)} \right|_{\epsilon=\epsilon_F} \frac{I_{21}}{I_{01}} \frac{T}{Z}, \tag{30}$$

where we again numerically compute the ratio of the integrals $I_{21}/I_{01} = 2.65$. A similar expression was recently given by Palsson and Kotliar, who considered the thermopower in a doped Mott insulator.[16] The sign of the thermopower gives information on the type of charge carriers (electron or holes) that are contributing mostly to the transport. This sign comes in our expressions from the slope of the density of states at the Fermi energy.

The ratio of the thermopower to the specific heat at low temperatures is given by

$$\frac{S(T)}{\gamma T} = -\frac{1}{|e|} \frac{3}{2\pi^2} \left. \frac{\partial D_0(\epsilon)/\partial \epsilon}{D_0(\epsilon)^2} \right|_{\epsilon=\epsilon_F} \frac{I_{21}}{I_{01}}, \tag{31}$$

which is universal, i.e., independent of the interactions for a given degree of frustration in the lattice.

A simpler expression for the slope of the thermopower can be found in the limit $t_2^*/t_1^* \to 0$; in this case, expression (9) reduces to

$$S(T) \approx \frac{-k_B}{|e|} \frac{I_{21}}{I_{01}} \sqrt{2} \frac{t_2^*}{Z t_1^{*2}} T. \tag{32}$$

The slope of the thermopower is, therefore, directly proportional to the degree of frustration present in the frustrated hypercubic lattice. We have checked that at low temperatures our numerical results are in good agreement with this expression.

The simple expression (31) may explain the huge values ($S > k_B/e$ at 300 K) recently observed[48] for $NaCo_2O_4$, which has potential applications as a thermoelectric material.[49] This material consists of layers of CoO_2 with the crystal structure of a triangular lattice. For such a lattice the noninteracting density of states can be expressed analytically as shown in Ref. 50. Evaluating the derivative at the Fermi energy for a half-filled band gives

$$\left. \frac{\partial D_0(\epsilon)/\partial \epsilon}{D_0(\epsilon)^2} \right|_{\epsilon=\epsilon_F} = -1.24 \tag{33}$$

and so Eq. (31) predicts a ratio of $1/2|e|$, which reexpressed in appropiate units is 5.23×10^{-3} μ V mol/mJ. The measured thermopower is approximately linear in temperature up to about $T = 200$ K, at which it has a value of about 80 μV/K. The measured specific heat coefficient[51] is $\gamma = 48$ mJ/(mol K^2) giving a ratio $S(T)/\gamma T$ of 8×10^{-3} μV mol/mJ. This suggests that the large value of the thermopower of this material is not just due to strong correlations enhancing the effective mass but also due to the large particle-hole asymmetry associated with the triangular lattice. Also, the theory presented predicts a positive thermopower at low temperatures for the triangular lattice, consistent with experiment.[48]

C. Hall resistance

In the low-temperature limit, the Hall conductivity (8) reduces to

$$\sigma_{xy}^H = \frac{\sigma_0^H}{2d^2} \frac{3}{8\pi^2} D_0(\epsilon = \epsilon_F) \frac{\epsilon_F}{C^2 T^4} I_{02} \tag{34}$$

where the integral I_{02} is defined by Eq. (25) and is equal to 0.007 30. This expression depends on the interaction through $C \propto 1/Z^2$. A similar expression was recently found by Lange and Kotliar.[17]

The Hall coefficient reduces at low temperatures to

$$R_H \approx \frac{a^3}{6|e|} \frac{I_{02}}{I_{01}^2} \frac{\mu - \mathrm{Re}\,\Sigma(\omega=\mu)}{t_1^{*2} D_0(\epsilon_F)} \tag{35}$$

where $I_{02}/I_{01}^2 = 1.06$. Expression (35) shows temperature dependence through the chemical potential $\mu = \mu(T)$. At $T = 0$, expression (35) is independent of U because from Luttinger's theorem $\epsilon_F \equiv \mu - \mathrm{Re}\,\Sigma(\omega=\mu)$. Moreover, in the $U \to 0$ limit, and in the particle-hole symmetric case, expression (35) reduces to zero, $R_H = 0$ for $T \to 0$, as it should, as the density of holes cancels exactly the density of electrons

contributing to the transport in the system. As soon as the degree of frustration $t_2^*/t_1^* \neq 0$, then, the Hall coefficient is nonzero, and, again at $T=0$, independent of the Coulomb interaction. The sign of the Hall coefficient depends on the sign of the real part of the self-energy referred to the chemical potential. This means that, in general, it is possible to have a different sign for the thermopower and the Hall factor at low temperatures depending on the shape of the bare density of states and the Fermi energy.

D. Optical conductivity

At low temperatures the optical conductivity (7) reduces to

$$\sigma(\omega)=\frac{\sigma_0 D(\epsilon_F)}{d\pi}\int d\nu \frac{f(\nu)-f(\nu+\omega)}{\omega} \times \frac{[1/\tau(\nu)+1/\tau(\nu+\omega)]}{(\omega/Z)^2+\frac{1}{4}[1/\tau(\nu)+1/\tau(\nu+\omega)]^2}, \quad (36)$$

where $1/\tau(\nu)=2\,\mathrm{Im}\,\Sigma(\nu)$, similar to an expression first obtained by Murata.[52] For $\omega \ll \pi T$, the frequency dependence of the self-energy can be neglected and the above expression reduces to

$$\sigma(\omega,T)=\frac{2\sigma_0 D_0(\epsilon_F)Z}{d\pi}\frac{\tau^*(T)}{1+[\omega\tau^*(T)]^2}, \quad (37)$$

where $1/\tau(T)=2\,\mathrm{Im}\,\Sigma(0,T)\approx 2C(\pi T)^2$ and $\tau^*(T)=\tau(T)/Z$.

IV. CROSSOVER TO INCOHERENT EXCITATIONS

The Fermi liquid behavior discussed in the previous section occurs only up to some temperature of the order of the coherence temperature T_0. There is then a smooth crossover to the case where all of the low-energy excitations are incoherent (see Fig. 1). In this section we present results showing the effect of this crossover on transport properties.

A. Resistivity

The temperature dependence of the resistivity is shown in Fig. 3 for $t_2^*/t_1^*=0.1$ and various interaction strengths. It has two properties often observed in strongly correlated metals: (i) for strong interactions a nonmonotonic temperature dependence occurs, and (ii) for high temperatures it smoothly increases to large values corresponding to mean free paths less than a lattice constant.

For values of the interaction comparable to the bandwidth, $U\approx 4t_1^*$, the resistivity shows a peak at a temperature of about $0.2t_1^*$. The temperature at which this peak appears corresponds approximately to the temperature at which there are no longer Fermi liquid quasiparticles present (see Fig. 1). The decreasing resistance with increasing temperature, characteristic of a semiconductor or insulator, is due to thermal excitations to the upper Hubbard band. Note that the peak temperature is not the Kondo temperature, which in our calculations is at much lower temperatures. Such a peak in the resistivity is observed in heavy fermion sytems[5] and some of the κ-(BEDT-TTF)$_2X$ family of organic superconductors.[9] Results similar to Fig. 3 were obtained previously for the simple hypercubic lattice ($t_2=0$) when the impurity problem was solved using quantum Monte Carlo calculations and the noncrossing approximation,[25] and for the Bethe lattice when the impurity problem was solved using iterative perturbation theory.[53]

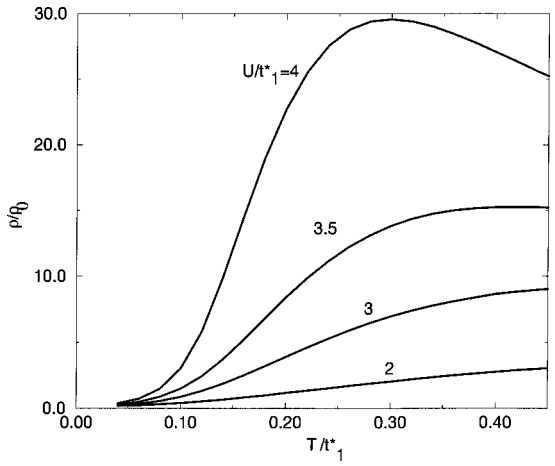

FIG. 3. Temperature dependence of the resistivity in the frustrated hypercubic lattice for $t_2^*/t_1^*=0.1$ and for different values of $U/t_1^*=2$, 3, 3.5, and 4. For $U=4t_1^*$ there is a crossover from metallic behavior at low temperatures to insulating behavior at high temperatures. The resistivity is given in units of $\rho_0=\hbar a/e^2$, where a is a lattice constant which corresponds to a value of the resistivity at which the mean free path is comparable to a lattice constant.

Bad metals. In conventional metals transport occurs by well-defined quasiparticles; they have a wavelength ($\sim 1/k_F$) much less than the mean free path l and so transport properties can be described by the Boltzmann equation. However, if the scattering is sufficiently strong that the mean free path is comparable to a lattice constant ($l\sim a$) then $k_F l \sim \pi$ and the quasiparticle concept breaks down. This is often referred to as the Mott-Ioffe-Regel limit.[54] For an isotropic three-dimensional metal this corresponds to a conductivity of $\sigma=e^2/(3\hbar a)$, and is sometimes referred to as the Mott minimum conductivity. However, for a wide range of strongly correlated metals, including the cuprates,[55] fullerene metals (A_3C_{60}),[56] the organic superconductors κ-(BEDT-TTF)$_2X$,[9] Sr_2RuO_4,[57] $SrRuO_3$,[58] and VO_2,[59] it is observed that as the temperature increases the resistivity can increase to values corresponding to mean free paths much less than a lattice constant. Such materials have been referred to as ''bad metals.''[60] In contrast, in the A-15 metals the resistivity appears to 'saturate' at a high-temperature value corresponding to the Mott-Ioffe-Regel limit.[61] However, it has recently been suggested that the resistivity does not saturate but rather a change in temperature dependence occurs when the scattering is strong enough to cause a breakdown of the Migdal approximation.[62] Emery and Kivelson proposed[60] that the smooth temperature dependence of the resistance in bad metals suggests that the low-temperature transport is also not due to quasiparticles.

At low temperatures the resistivity given by (24) can be written

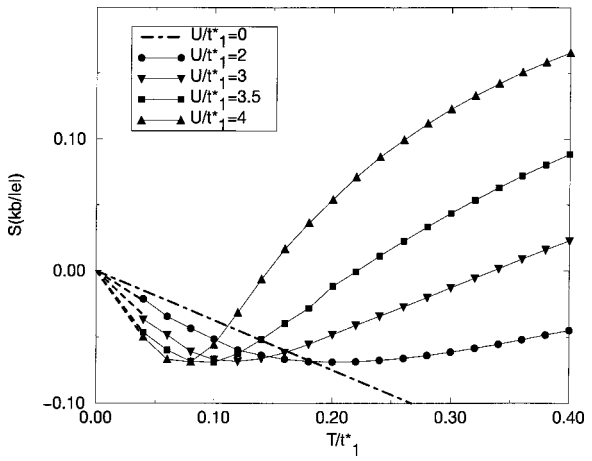

FIG. 4. Temperature dependence of the thermopower for the frustrated hypercubic lattice for $t_2^*/t_1^*=0.1$ and for different values of $U/t_1^*=2$, 3, 3.5, and 4. The dashed lines are based on linear extrapolations to zero temperature as expressed in Eq. (32). The curves show how interactions between electrons significantly change the magnitude and temperature dependence from the linear behavior expected for a weakly interacting Fermi liquid. Indeed, the appearance of a minimum in the thermopower is a signature of thermal destruction of the coherent Fermi liquid state that exists at low temperatures.

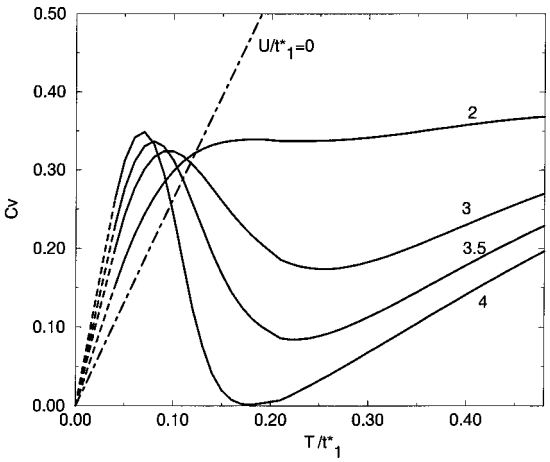

FIG. 5. Specific heat in units of the gas constant R, for the frustrated hypercubic lattice for $t_2^*/t_1^*=0.1$ and for different values of $U/t_1^*=2$, 3, 3.5, and 4. Note that the peak occurs at a temperature comparable to that at which the peak in the thermopower occurs (compare with Fig. 4). The dashed lines are linear extrapolations to zero temperature. As in the case of the thermopower, the simple linear behavior found for the noninteracting case is qualitatively changed and a peak at low temperatures shows up for $U/t_1^* \geqslant 3$. The temperature scale at which this peak appears is set by the binding energy of the spin-screening cloud formed at each lattice site due to the Kondo effect.

$$\rho \simeq d(2\pi)^{1/2}\frac{\hbar a}{e^2}\frac{1}{\tau D}, \tag{38}$$

where τ is the scattering time. The Mott-Ioffe-Regel condition ($l \simeq a$) is equivalent to $\tau D \simeq 2\pi$, leading to a resistivity

$$\rho_0 \simeq \frac{\hbar a}{e^2}. \tag{39}$$

For $a=10$ Å this corresponds to a resistivity of 3 mΩ cm. Figure 3 shows that even for moderate interaction strengths the resistivity can smoothly increase to values much larger than this. Furthermore, our results provide a counterexample to the ideas of Emery and Kivelson[60] since there is a smooth crossover from transport by incoherent excitations at high temperatures to Fermi liquid transport at low temperatures.

B. Thermopower

In Fig. 4, we show the results for the thermopower as a function of temperature for different values of the Coulomb interaction U and in the nearly symmetric case $t_2^*/t_1^*=0.1$.

The low-temperature behavior is correctly described by Eq. (9). As can be observed, the slope of the thermopower at low temperatures increases with increasing U, scaling as the effective mass $m^*/m=1/Z$. We find a minimum in the thermopower which is rather shallow for small U and becomes increasingly pronounced with increasing U. A similar feature also occurs for doped Mott insulators[13] and for the Anderson lattice.[19] We observe that the mimimum moves to higher temperatures as U/t_1^* is decreased. This is a consequence of the increase in the Kondo scale with decreasing U and is supported by the observation that this minimum follows the peak in the specific heat. To illustrate the close relationship between the thermopower and the specific heat, Fig. 5 shows the specific heat for the same parameter values as Fig. 4.

The peak in the specific heat, already analyzed by several authors,[63] is associated with the binding energy of the Kondo spin screening cloud which eventually forms at each lattice site. The high-temperature behavior found is typical of systems that have a depleted density of states at the Fermi energy, for example, in semimetals and insulators one expects the magnitude of the thermopower to decrease as the temperature is decreased. This is more easily understood from the behavior of the spectral densities which show this effective depletion of quasiparticle excitations at the Fermi energy (see Fig. 1).

The change in sign of the thermopower at intermediate temperatures $T \approx 0.2t_1^*$ for $U=3.5t_1^*$ can be explained from the fact that the spectral weight of the quasiparticle excitations is transferred mostly to the lower rather than to the upper Hubbard band, making the holes, rather than the electrons, the dominant carriers contributing to energy transport (see Fig. 1).

It is worth stressing that it is not necessary to get to too large values of U/t_1^* to find a clear signature of the minimum in the thermopower and strong temperature behavior. This is a feature that one can find in sufficiently correlated systems far from the Mott transition as can be checked from the effective masses we obtain, m^*/m, which in our calculations vary between 2 and 4 for $U \approx 2$ and 4, respectively.

Figure 6 shows the thermopower when the frustration is increased to $t_2^*/t_1^*=0.3$. The magnitude of the thermopower is enhanced as a result of the larger asymmetry present in the particle-hole excitations of the system. Thus, the slope at low temperatures is increased by a factor of about 3, as expected from Eq. (32). The main features remain similar to the less frustrated case $t_2^*/t_1^* \approx 0.1$, although the minimum of the thermopower is more pronounced for a larger degree of frustration.

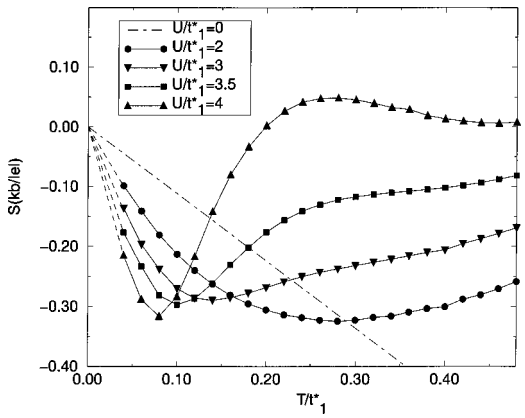

FIG. 6. Temperature dependence of the thermopower for the frustrated hypercubic lattice with $t_2^*/t_1^*=0.3$ and $U/t_1^*=2$, 3, 3.5, and 4. The dashed lines are extrapolations to zero temperature. The effect of frustration is more clearly seen when comparing this figure with the case $t_2^*/t_1^*=0.1$. The values of the thermopower are increased as well as the slope at low temperatures. However, the position of the minimum is nearly independent of the degree of frustration.

The thermopower of the cuprates[64] and the organic superconductors κ-(BEDT-TTF)$_2X$ (Ref. 65) and β-(BEDT-TTF)$_2X$ (Ref. 66) has the common properties that it is not a monotonic function of temperature and has large values of order 10–50 μV/K at 100 K. For the organics these properties cannot be explained in terms of the calculated band structures and a weakly interacting Fermi liquid.[65,66] For Sr_2RuO_4 the thermopower increases nonlinearly with temperature from 4 K to 300 K, appearing to saturate at high temperatures, and has the opposite sign to the Hall coefficient.[67]

As discussed above a peak or minimum in the thermopower is a signature of the decay of coherent excitations with increasing temperature. It is desirable to see if this feature can be observed in experiments on other strongly correlated metals. Such a peak should be clearly distinguishable from a peak due to phonon drag[68] by several features. The latter produces a thermopower that is proportional to the lattice specific heat and thus cubic in the temperature for $T \ll \theta_D$. For higher temperatures the phonon drag thermopower goes like $1/T$. The result is a peak around a temperature of $(0.1–0.2)\,\theta_D$. Values of θ_D can be deduced from the specific heat data. Thus, it should be possible to distinguish whether an observed peak in a material is due to phonon drag or loss of Fermi liquid coherence because of the different temperatures at which they occur and because of the different behavior at higher temperatures.

Zhou and Goodenough have observed peaks around 100 K in the thermopower of $CaVO_3$ (Ref. 69) and $La_{1-x}Nd_xCuO_3$.[70] They attribute these peaks to phonon drag. This peak cannot be due to the correlation effects considered here because it occurs at too low a temperature. In $CaVO_3$ the optical conductivity still has a Drude peak at 300 K,[71] and it is estimated that $D=1$ eV and $U=3$ eV. Consequently, the coherence temperature will be of the order of 1000 K.

The peak in the electronic specific heat would be extremely difficult to observe because it will be masked by the T^3 phonon contribution. In contrast, the phonon contribution to the thermopower decreases with increasing temperature and so should not mask the feature due to correlations.

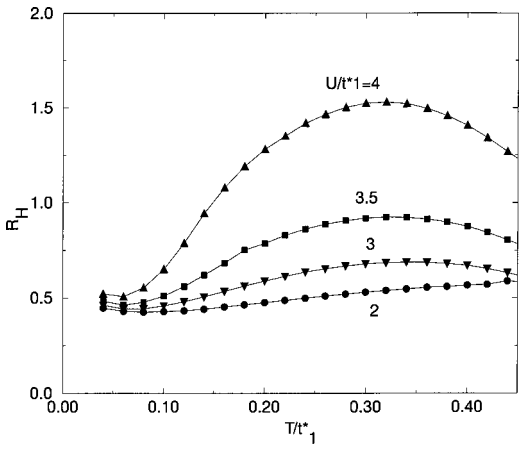

FIG. 7. Temperature dependence of the Hall coefficient for the frustrated hypercubic lattice with $t_2^*/t_1^*=0.1$ and for different values of $U/t_1^*=2$, 3, 3.5, and 4. Note the saturation of the Hall coefficient at low temperatures for all values of U/t_1^*. As the interaction is increased strong temperature dependence arises.

C. Hall resistance

In Figs. 7 and 8 we show results for the temperature dependence of the Hall coefficient R_H for $t_2^*/t_1^*=0.1$ and 0.3, respectively. We observe from the curves that for small values of the U/t_1^* ratio, the Hall coefficient is nearly independent of temperature, whereas for larger values of the interaction there is an increase in the Hall coefficient for increasing T reaching a maximum at $T\approx 0.3t_1^*$. This fact is observed for both values of the frustration shown. Note that the sign of the Hall coefficient is not necessarily the same as the sign of the thermopower.

For a given value of the frustration, all curves converge to the same value at $T=0$ as expected from Eq. (35). However,

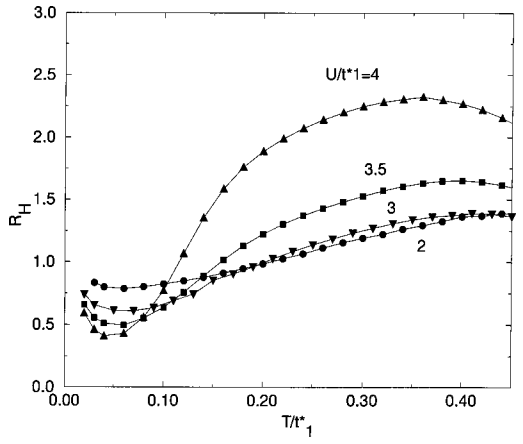

FIG. 8. Temperature dependence of the Hall coefficient for the frustrated hypercubic lattice with $t_2^*/t_1^*=0.3$ and for different values of $U/t_1^*=2$, 3, 3.5, and 4. A greater degree of asymmetry can enhance some features of the Hall resistance. At low temperatures, it is more strongly temperature dependent than for $t_2^*/t_1^*=0.1$ and an upturn in the Hall coefficient can even arise.

the temperature dependence at low temperatures for $t_2^*/t_1^* = 0.3$ differs from the $t_2^*/t_1^* = 0.1$ case. The behavior at low temperatures is determined by the temperature dependence of the chemical potential, which depends on the lattice analyzed through the bare density of states and the value of U/t_1^*. For the case $t_2^*/t_1^* = 0.3$, the Hall coefficient is more strongly dependent on U than for the $t_2^*/t_1^* = 0.1$ case. Moreover, an upturn of the Hall coefficient is found in the low-temperature limit $T \to 0$ in the latter case. This means that, although qualitatively the situation is similar for different degrees of frustration, some features can be enhanced and may depend on the details of the band structure and the bare density of states of the material.

The Hall coefficient for a doped Mott insulator on a simple hypercubic lattice was calculated previously by Pruschke *et al.*[13] and Lange and Kotliar[17] using dynamical mean-field theory and found to have a qualitatively similar temperature dependence.

The layered perovskite Sr_2RuO_4 has Fermi liquid properties at low temperatures[8] but the Hall resistance of Sr_2RuO_4 is strongly temperature dependent.[72] It has a value of about -1.15×10^{-10} m^3 C^{-1} below 1 K and then increases rapidly with temperature and changes sign around 35 K and saturates at high temperatures to a value of about -0.1×10^{-10} m^3 C^{-1}. The behavior and value below 1 K can be explained within a Fermi liquid picture.[72] However, the sign change can only be explained if the temperature dependence of the scattering rate in the different bands is significantly different.[73] An alternative explanation for the temperature dependence is the decay of coherence discussed here.

Experiments on organic metals κ-(BEDT-TTF)$_2X$ show a temperature-dependent Hall coefficient.[74] For β-(BEDT-TTF)$_2$I$_3$ the Hall resistance has a broad maximum around 40 K.[75]

D. Optical conductivity

Figure 9 shows the frequency-dependent conductivity calculated for our model with $U = 4t_1^*$ and $t_2^* = 0.1t_1^*$ at three different temperatures. It shows the important features noted below for a range of strongly correlated metals: (i) the Drude peak only exists at low temperatures, and (ii) most of the spectral weight is contained in broad high-energy features. Similar features were found previously using dynamical mean-field theory and exact diagonalization and iterated perturbation theory,[71,53] and for doped Mott insulators using quantum Monte Carlo calculations.[76]

Infrared measurements[77–79] of the frequency-dependent conductivity $\sigma(\omega)$ of κ-(BEDT-TTF)$_2X$ deviate from the Drude behavior found in conventional metals. At room temperature $\sigma(\omega)$ is dominated by a broad peak around 300 or 400 meV (depending on the polarization and anion X) with a width of about 150 meV. Even down to 50 K no Drude-like peak at zero frequency is present (see Fig. 2 in Ref. 9). At 25 K the high-energy peak decreases slightly in temperature and a Drude-like peak appears but can only be fitted to a Drude form if the scattering rate and effective mass are frequency dependent.[77] Similar results are obtained for α-(BEDT-TTF)$_2$NH$_4$Hg(SCN)$_4$.[80]

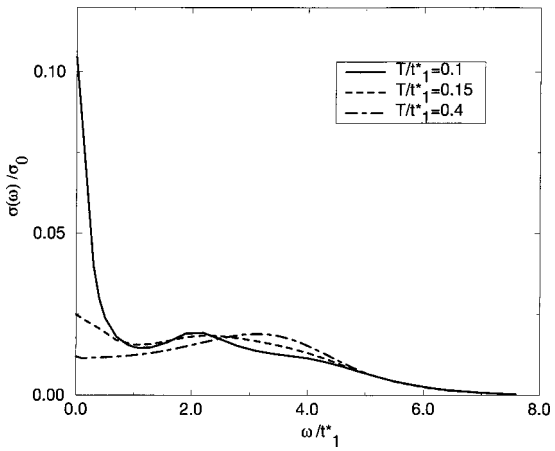

FIG. 9. Strong temperature dependence of the optical conductivity. The curves shown are for $U = 4t_1^*$, $t_2^* = 0.1t_1^*$, at three different temperatures. A Drude peak at zero frequency only occurs at low temperatures. The feature around $\omega \approx U/2$ is due to transitions from the coherent quasiparticle band at the Fermi energy to the upper Hubbard band and from the lower Hubbard band to the quasiparticle band. The broad feature at $\omega \approx U$ at higher temperatures is due to transitions from the lower to the upper Hubbard band (compare Fig. 1). Note that most of the spectral weight is contained in the high-frequency features.

Experiments on β-(BEDT-TTF)$_2X$ where $X = I_3$, IBr_2, and AuI_2 at 30 K show no Drude peak.[81] Experiments on β''-(BEDT-TTF)$_2SF_5CH_2CF_2SO_3$ show no Drude peak, even down to 14 K.[82] Furthermore, it does not appear that the spectral weight is conserved as the temperature varies.

For $(TMTSF)_2PF_6$ at 20 K there is a Drude peak and a broad peak around 200 cm^{-1}.[83] The Drude peak contains less than one percent of the total spectral weight and is not present at 100 K. The Drude peak has been fitted to a generalized Drude form with a frequency-dependent scattering rate $1/\tau(\omega) \sim \omega^2$, given by a phenomenological form used previously for the heavy fermion compound UPt_3.

For $SrRuO_3$ a Drude peak was observed at 40 K but not above about 100 K.[84] The conductivity $\sigma(\omega) \sim 1/\omega^{1/2}$ above a temperature-dependent crossover frequency of about $3k_BT/\hbar$, whereas in conventional metals, $\sigma(\omega) \sim 1/\omega^2$. The low-temperature Drude peak could be fitted to a generalized Drude form with $1/\tau(\omega) \sim \omega$.

V. CONCLUSIONS

In order to gain a better understanding of why the transport properties of strongly correlated metals deviate significantly from the properties of elemental metals the transport properties of a specific Hubbard model were calculated. The transport properties are strongly temperature dependent because as the temperature increases there is a smooth crossover from coherent Fermi liquid excitations to incoherent excitations. This leads to a nonmonotonic temperature dependence for the resistance, thermopower, and Hall coefficient. The resistance smoothly increases from a quadratic temperature dependence at low temperatures, obeying the Kadowaki-Woods rule, to large values characteristic of a bad metal. Further signatures of the thermal destruction of quasiparticle excitations are a peak in the thermopower and the

absence of a Drude peak in the optical conductivity.

The results presented here are qualitatively similar to the observed transport properties of a wide range of strongly correlated metals, including transition metal oxides, strontium ruthenates, and organic metals. For example, the physical picture presents a natural explanation of the recently presented puzzle[85,84] of the properties of $SrRuO_3$. Although Shubnikov–de Haas oscillations, with a Fermi liquid temperature dependence, were observed at low temperatures,[85] it was found that the optical conductivity deviated significantly from a Drude form[84] and it is a bad metal at high temperatures.[57] This is because the latter measurements involve energy scales (in frequency and/or temperature) much larger than the coherence temperature associated with Fermi liquid excitations.

Finally, it is particularly desirable that measurements of the temperature dependence of the thermopower be made on a wide range of materials because the peak that we find represents a well-defined signature of the thermal destruction of quasiparticle excitations. Furthermore, measurements on a single material of *all* the transport properties calculated here are needed in order to provide a comprehensive test of the physical picture presented. Ideal candidate materials, since they are metallic at ambient temperature and have coherence temperatures of the order of 50–100 K, are Sr_2RuO_4, κ-$(BEDT\text{-}TTF)_2Cu(SCN)_2$, and β-$(BEDT\text{-}TTF)_2IBr_2$. A quantitative comparison of theory with experiment will require that the theory presented here be modified to include the effects of band structure.[86]

ACKNOWLEDGMENTS

This work was supported by the Australian Research Council. We thank W. Krauth, A. Levy-Yeyati, F. Flores, G. Kotliar, A. Georges, and M. J. Rozenberg for helpful discussions. Some of the computer codes used were taken from Ref. 12.

*Electronic address: merino@phys.unsw.edu.au
†Electronic address: ross@phys.unsw.edu.au

[1] For a review, see P. Fulde, *Electron Correlations in Molecules and Solids*, 3rd enlarged ed. (Springer-Verlag, Berlin, 1995).
[2] F. Gebhardt, *The Mott Metal-Insulator Transition* (Springer-Verlag, Berlin, 1997).
[3] For a recent experimental review, see W.Y. Liang, J. Phys.: Condens. Matter **10**, 11 365 (1998).
[4] M. Imada, A. Fujimori, and Y. Tokura, Rev. Mod. Phys. **70**, 1039 (1998).
[5] G.R. Stewart, Rev. Mod. Phys. **56**, 755 (1984).
[6] D.L. Cox and N. Grewe, Z. Phys. B: Condens. Matter **71**, 321 (1988).
[7] L. Degiorgi, Rev. Mod. Phys. **71**, 687 (1999).
[8] Y. Maeno, K. Yoshida, H. Hashimoto, S. Nishizaki, S. Ikeda, M. Nohara, T. Fujita, A.P. MacKenzie, N.E. Hussey, J.G. Bednorz, and F. Lichtenberg, J. Phys. Soc. Jpn. **66**, 1405 (1997).
[9] R.H. McKenzie, Comments Condens. Matter Phys. **18**, 309 (1998).
[10] C. Bourbonnais and D. Jerome, cond-mat/9903101 (unpublished).
[11] D. Vollhardt, in *Perspectives in Many-Particle Physics*, Proceedings of the International School of Physics, ''Enrico Fermi,'' Course CXXI, edited by R. A. Broglia and J. R. Schrieffer (North-Holland, Amsterdam, 1994), p. 31.
[12] A. Georges, G. Kotliar, W. Krauth, and M.J. Rozenberg, Rev. Mod. Phys. **68**, 13 (1996).
[13] Th. Pruschke, M. Jarrell, and J. Freericks, Adv. Phys. **44**, 187 (1995).
[14] O. Parcollet and A. Georges, Phys. Rev. B **59**, 5341 (1999).
[15] M.S. Laad, L. Craco, and E. Müller-Hartmann, cond-mat/9907328 (unpublished).
[16] G. Palsson and G. Kotliar, Phys. Rev. Lett. **80**, 4775 (1998).
[17] E. Lange and G. Kotliar, Phys. Rev. B **59**, 1800 (1999).
[18] E. Muller-Hartmann, Z. Phys. B: Condens. Matter **74**, 507 (1989).
[19] H. Schweitzer and G. Czycholl, Phys. Rev. Lett. **67**, 3724 (1991).
[20] M.H. Hettler, M. Mukherjee, M. Jarrell, and H.R. Krishnamurthy, cond-mat/9903273 (unpublished); Th. Maier, M. Jarrell, Th. Pruschke, and J. Keller, cond-mat/9906253 (unpublished).
[21] A. Khurana, Phys. Rev. Lett. **64**, 1990 (1990).
[22] B.S. Shastry, B.I. Shraiman, and R.R.P. Singh, Phys. Rev. Lett. **70**, 2004 (1993).
[23] P. Majumdar and H.R. Krishnamurthy, cond-mat/9512151 (unpublished).
[24] A. C. Hewson, *The Kondo Problem to Heavy Fermions* (Cambridge University Press, Cambridge, 1993).
[25] Th. Pruschke, D. Cox, and M. Jarrell, Phys. Rev. B **47**, 3553 (1993).
[26] H. Kajueter and G. Kotliar, Phys. Rev. Lett. **77**, 131 (1996).
[27] A. Martin-Rodero, F. Flores, M. Baldo, and R. Pucci, Solid State Commun. **44**, 911 (1986).
[28] M. Potthoff, T. Wegner, and W. Nolting, Phys. Rev. B **55**, 16 132 (1997).
[29] K. Fischer, cond-mat/9903245 (unpublished).
[30] E. Muller-Hartmann, Z. Phys. B: Condens. Matter **76**, 211 (1989).
[31] H. Schweitzer and G. Czycholl, Z. Phys. B: Condens. Matter **79**, 377 (1990).
[32] K. Yamada, Prog. Theor. Phys. **55**, 1345 (1976).
[33] R. Bulla, A.C. Hewson, and Th. Pruschke, J. Phys.: Condens. Matter **10**, 8365 (1998).
[34] D. Meyer, T. Wegner, M. Potthoff, and W. Nolting, Physica B **270**, 225 (1999).
[35] A. Levy-Yeyati, A. Martin-Rodero, and F. Flores, Phys. Rev. Lett. **71**, 2991 (1993).
[36] W. H. Press, S. A. Teukolsky, W. T. Vetterling, and B. P. Flannery, *Numerical Recipes in Fortran*, 2nd ed. (Cambridge University Press, Cambridge, 1992), p. 382.
[37] H.J. Vidberg and J.W. Serene, J. Low Temp. Phys. **29**, 179 (1977).
[38] J. Wosnitza, *Fermi Surfaces of Low Dimensional Organic Metals and Superconductors* (Springer, Berlin, 1996).
[39] A.P. Mackenzie, S.R. Julian, A.J. Driver, G.J. McMullan, M.P. Ray, G.G. Lonzarich, Y. Maeno, S. Nishizaki, and T. Fujita, Phys. Rev. Lett. **76**, 3786 (1996).
[40] K. Yamada and K. Yosida, Prog. Theor. Phys. **76**, 621 (1986).
[41] G. Uhrig and D. Vollhardt, Phys. Rev. B **52**, 5617 (1995).
[42] K. Kadowaki and S.B. Woods, Solid State Commun. **58**, 507 (1986).
[43] K. Miyake, T. Matsuura, and C.M. Varma, Solid State Commun. **71**, 1149 (1989).

[44] Y. Tokura, Y. Taguchi, Y. Okada, Y. Fujishima, T. Arima, K. Kumagai, and Y. Iye, Phys. Rev. Lett. **70**, 2126 (1993).
[45] B. Andraka, R. Pietri, S.G. Thomas, G.R. Stewart, E.W. Scheidt, and T. Schreiner, Eur. Phys. J. B **12**, 55 (1999).
[46] G. Moeller, Q. Si, G. Kotliar, and M. Rozenberg, Phys. Rev. Lett. **74**, 2082 (1995).
[47] A. Houghton, N. Read, and H. Won, Phys. Rev. B **35**, 5123 (1987).
[48] I. Terasaki, Y. Sasago, and K. Uchinokura, Phys. Rev. B **56**, R12 685 (1997).
[49] For a recent review of thermopower and potential thermoelectric materials, see G.D. Mahan, Solid State Phys. **51**, 81 (1997).
[50] V. Ivanov, K. Yakushi, and E. Ugolkova, Physica C **275**, 26 (1997).
[51] Y. Ando, N. Miyamoto, K. Segawa, T. Kawata, and I. Terasaki, Phys. Rev. B **60**, 10 580 (1999).
[52] K. Murata, Ph.D. thesis, Cornell University, 1970.
[53] M.J. Rozenberg, G. Kotliar, H. Kajueter, G.A. Thomas, D.H. Rapkine, J.M. Honig, and P. Metcalf, Phys. Rev. Lett. **75**, 105 (1995); M.J. Rozenberg, G. Kotliar, and H. Kajueter, Phys. Rev. B **54**, 8452 (1996).
[54] N. F. Mott, *Metal-Insulator Transitions*, 2nd ed. (Taylor & Francis, London, 1990), p. 30.
[55] M. Gurvitch and A.T. Fiory, Phys. Rev. Lett. **59**, 1337 (1987).
[56] A.F. Hebard, T.T.M. Palstra, R.C. Haddon, and R.M. Fleming, Phys. Rev. B **48**, 9945 (1993).
[57] A.W. Tyler, A.P. Mackenzie, S. Nishizaki, and Y. Maeno, Phys. Rev. B **58**, R10 107 (1998).
[58] L. Klein, Phys. Rev. Lett. **77**, 2774 (1996); P.B. Allen, H. Berger, O. Chauvet, L. Forro, T. Jarlborg, A. Junod, B. Revaz, and G. Santi, Phys. Rev. B **53**, 4393 (1996).
[59] P.B. Allen, R.M. Wentzcovitch, W.W. Schulz, and P.C. Canfield, Phys. Rev. B **48**, 4359 (1993).
[60] V.J. Emery and S.A. Kivelson, Phys. Rev. Lett. **74**, 3253 (1995); V.J. Emery, S.A. Kivelson, and V.N. Muthukumar, cond-mat/9901270 (unpublished).
[61] Z. Fisk and G.W. Webb, Phys. Rev. Lett. **36**, 1084 (1976).
[62] A.J. Millis, J. Hu, and S. Das Sarma, Phys. Rev. Lett. **82**, 2354 (1999).
[63] A. Georges and W. Krauth, Phys. Rev. B **48**, 7167 (1993).
[64] J.-S. Zhou and J.B. Goodenough, Phys. Rev. B **51**, 3104 (1995).
[65] R.C. Yu, J.M. Williams, H.H. Wang, J.E. Thompson, A.M. Kini, K.D. Carlson, J. Ren, M.H. Whangbo, and P.M. Chaikin, Phys. Rev. B **44**, 6932 (1991); L.I. Buravov, N.D. Kushch, V.A. Merzhanov, M.V. Osherov, A.G. Khomenko, and E.B. Yagubskii, J. Phys. I **2**, 1257 (1992); S.V. Demishev, M.V. Kondrin, V.V. Glushkov, N.E. Sluchanko, and N.A. Samarin, Zh. Éksp. Teor. Fiz. **114**, 323 (1998) [JETP **86**, 182 (1998)].
[66] T. Mori and H. Inokuchi, J. Phys. Soc. Jpn. **57**, 3674 (1988).
[67] H. Yoshino, K. Murata, N. Shirakawa, Y. Nishihara, Y. Maeno, and T. Fujita, J. Phys. Soc. Jpn. **65**, 1548 (1996).
[68] R. D. Barnard, *Thermoelectricity in Metals and Alloys* (Taylor & Francis, London, 1972).
[69] J.-S. Zhou and J.B. Goodenough, Phys. Rev. B **54**, 13 393 (1996).
[70] J.-S. Zhou, W. Archibald, and J.B. Goodenough, Phys. Rev. B **57**, R2017 (1998).
[71] M.J. Rozenberg, I.H. Inoue, H. Makino, F. Iga, and Y. Nishihara, Phys. Rev. Lett. **76**, 4781 (1996); H. Makino, I.H. Inoue, M.J. Rozenberg, I. Hase, Y. Aiura, and S. Onari, Phys. Rev. B **58**, 4384 (1998).
[72] A.P. Mackenzie, N.E. Hussey, A.J. Diver, S.R. Julian, Y. Maeno, S. Nishizaki, and T. Fujita, Phys. Rev. B **54**, 7425 (1996).
[73] I.I. Mazin, D.A. Papaconstantopoulos, and D.J. Singh, cond-mat/9907442 (unpublished).
[74] K. Murata, M. Ishibashi, Y. Honda, N.A. Fortune, M. Tokumoto, N. Kinoshita, and H. Anzai, Solid State Commun. **76**, 377 (1990); Yu.V. Sushko, N. Shirakawa, K. Murata, Y. Kubo, N.D. Kushch, and E.B. Yagubskii, Synth. Met. **85**, 1541 (1997); M.A. Tanatar, T. Ishiguro, H. Ito, M. Kubota, and G. Saito, Phys. Rev. B **55**, 12 529 (1997).
[75] B. Korin-Hamzić, L. Forró, and J.R. Cooper, Phys. Rev. B **41**, 11 646 (1990).
[76] M. Jarrell, J.K. Freericks, and Th. Pruschke, Phys. Rev. B **51**, 11 704 (1995).
[77] K. Kornelsen, J.E. Eldridge, C.C. Homes, H.H. Wang, and J.M. Williams, Solid State Commun. **72**, 475 (1989).
[78] J.E. Eldridge, K. Kornelsen, H.H. Wang, J.M. Williams, A.V. Strieby Crouch, and D.M. Watkins, Solid State Commun. **79**, 583 (1991).
[79] M. Tamura, H. Tajima, K. Yakushi, H. Kuroda, A. Kobayashi, R. Kato, and H. Kobayashi, J. Phys. Soc. Jpn. **60**, 3861 (1991).
[80] M. Dressel, J.E. Eldridge, H.H. Wang, U. Geiser, and J.M. Williams, Synth. Met. **52**, 201 (1992).
[81] C.S. Jacobsen, J.M. Williams, and H.H. Wang, Solid State Commun. **54**, 937 (1985); C.S. Jacobsen, D.B. Tanner, J.M. Williams, U. Geiser, and H.H. Wang, Phys. Rev. B **35**, 9605 (1987).
[82] J. Dong, J.L. Musfeldt, J.A. Schlueter, J.M. Williams, P.G. Nixon, R.W. Winter, and G.L. Gard, Phys. Rev. B **60**, 4342 (1999).
[83] A. Schwartz, M. Dressel, G. Grüuner, V. Vescoli, L. Degiorgi, and T. Giamarchi, Phys. Rev. B **58**, 1261 (1998).
[84] P. Kostic, Y. Okada, Z. Schlesinger, J.W. Reiner, L. Klein, A. Kapitulnik, T.H. Geballe, and M.R. Beasley, Phys. Rev. Lett. **81**, 2498 (1998).
[85] A.P. Mackenzie, J.W. Reiner, A.W. Tyler, L.M. Galvin, S.R. Julian, M.R. Beasley, T.H. Geballe, and A. Kapitulnik, Phys. Rev. B **58**, R13 318 (1998).
[86] For some recent work which combines dynamical mean-field theory with band structure calculations, see A.I. Lichtenstein and M.I. Katsnelson, Phys. Rev. B **57**, 6884 (1998).